usefulness of PVR as a tool in selecting the appropriate intervention for coronary heart disease, and should include a comparison with the findings of IVUS.

References

1. Moshage WE, Achenbach S, Seese B, Bachmann K, Kirchgeorg M. Coronary artery stenoses: Three-dimensional imaging with electrocardiographically triggered, contrast agent-enhanced, electron beam CT. *Radiology* 1995; **196:** 707–714.
2. Shimamoto R, Suzuki J, Nishikawa J, Fujimori Y, Nakamura F, Shin WS, et al. Measuring the diameter of coronary arteries on MR angiograms using spatial profile curves. *AJR Am J Roentgenol* 1998; **170:** 889–893.
3. Nakanishi T, Kohata M, Miyasaka K, Fukuoka H, Ito K, Imazu M. Virtual endoscopy of coronary arteries using contrast-enhanced ECG triggered electron beam CT data sets. *AJR Am J Roentgenol* 2000; **174:** 1345–1347.
4. Beaulieu CF, Jefferey RB Jr, Karadi C, Paik DS, Napel S. Display modes for CT colonography: Part II. Blinded comparison of axial CT and virtual endoscopic and panoramic endoscopic volume-rendered studies 1. *Radiology* 1999; **212:** 203–212.
5. Neri E, Caramella D, Falaschi F, Sbragia P, Vignali C, Laiolo E, et al. Virtual CT intravascular endoscopy of the aorta: Pierced surface and floating shape thresholding artifacts 1. *Radiology* 1999; **212:** 276–279.
6. Rubin GD, Beaulieu CF, Argiro V, Ringl H, Norbash AM, Feller JF, et al. Perspective volume rendering of CT and MR images: Applications for endoscopic imaging. *Radiology* 1996; **199:** 321–330.
7. Achenbach S, Moshage W, Ropers D, Nossen J, Daniel WG. Value of electron-beam computed tomography for the noninvasive detection of high-grade coronary-artery stenoses and occlusions. *N Engl J Med* 1998; **339:** 1964–1971.
8. Achenbach S, Moshage W, Ropers D, Bachmann K. Comparison of vessel diameters in electron beam tomography and quantitative coronary angiography. *Int J Card Imaging* 1998; **14:** 1–7.
9. Funabashi N, Rubin GD, Kobayashi Y, Shifrin RY, Wexler L, Perlroth M. Accuracy of coronary artery dimensions with Electron-Beam CT angiography: Comparison of measurement methods. *Radiology* 1999; **213**(P): 269.
10. Brown DL, George CJ, Steenkiste AR, Cowley MJ, Leon MB, Cleman MW, et al. High-speed rotational atherectomy of human coronary stenoses: Acute and one-year outcomes from the new approaches to coronary intervention (NACI) registry. *Am J Cardiol* 1997; **80:** 60K–67K.
11. Funabashi N, Matsumoto A, Yoshida T, Watanabe S, Misumi K, Masuda Y. Usefulness of three-dimensional visualization of coronary arteries using electron-beam computed tomography data with volume rendering. *Jpn Circ J* 2000; **64:** 644–646.
12. Agatson AS, Janowitz WR, Hildner FJ, Zusmer NR Jr, Viamonte M, Detrano R. Quantification of coronary artery calcium using ultrafast computed tomography. *J Am Coll Cardiol* 1990; **15:** 827–832.

Heat Shock Transcription Factor 1 Protects Cardiomyocytes From Ischemia/Reperfusion Injury

Yunzeng Zou, MD, PhD*; Weidong Zhu, MD, PhD*; Masaya Sakamoto, MD; Yingjie Qin, MD; Hiroshi Akazawa, MD; Haruhiro Toko, MD, PhD; Miho Mizukami, MD; Norihiko Takeda, MD; Tohru Minamino, MD, PhD; Hiroyuki Takano, MD, PhD; Toshio Nagai, MD, PhD; Akira Nakai, MD, PhD; Issei Komuro, MD, PhD

Background—Because cardiomyocyte death causes heart failure, it is important to find the molecules that protect cardiomyocytes from death. The death trap is a useful method to identify cell-protective genes.

Methods and Results—In this study, we isolated the heat shock transcription factor 1 (HSF1) as a protective molecule by the death trap method. Cell death induced by hydrogen peroxide was prevented by overexpression of HSF1 in COS7 cells. Thermal preconditioning at 42°C for 60 minutes activated HSF1, which played a critical role in survival of cardiomyocytes from oxidative stress. In the heart of transgenic mice overexpressing a constitutively active form of HSF1, ischemia followed by reperfusion-induced ST-segment elevation in ECG was recovered faster, infarct size was smaller, and cardiomyocyte death was less than wild-type mice. Protein kinase B/Akt was more strongly activated, whereas Jun N-terminal kinase and caspase 3 were less activated in transgenic hearts than wild-type ones.

Conclusions—These results suggest that HSF1 protects cardiomyocytes from death at least in part through activation of Akt and inactivation of Jun N-terminal kinase and caspase 3. **(*Circulation*. 2003;108:3024-3030.)**

Key Words: ischemia ■ reperfusion ■ survival

Because the loss of functional cardiomyocytes causes heart failure, it is important to find the molecules that protect cardiomyocytes from death. The death trap is a useful method to identify cell-protective genes.[1] After transfection of the cDNA library constructed using cardiac mRNA in the mammalian expression vector, COS7 cells were cultured with a lethal dose of H_2O_2. We isolated several cDNAs from the surviving cells, and one of them was the heat shock transcription factor 1 (HSF1). The HSF family (HSF1-4) regulates the transcription of heat shock protein (HSP) genes.[2,3] In higher eukaryotes, expression of HSP genes is regulated primarily by HSF1 and HSF3 in response to various stresses and by HSF2 during development, whereas HSF4 seems to lack the activity as a positive transactivator. As a classical stress-responsive factor, HSF1 binds to heat shock element (HSE), which is present upstream of many HSP genes, and activates transcription of HSP genes under stress conditions. HSPs have been reported to be induced in various cardiovascular diseases and to have protective roles against various stresses.[4–6] Although HSF1 has also been reported to be expressed in hearts,[7] its role remains unknown. In the present study, using the transgenic mice expressing the active form of HSF1 (ΔHSF1),[8] we examined the role of HSF1 in the heart subjected to ischemia/reperfusion injury.

Methods

Materials

[γ-^{32}P]ATP was purchased from Du Pont-New England Nuclear Co. DMEM and FBS were from GIBCO BRL Co. pCMV SPORT heart cell expression cDNA library was from Life Technologies. The enhanced chemiluminescence reaction system was from Amersham. Other reagents were from Sigma.

Cloning of Cardioprotective Genes by Death Trap Method

COS7 cells cultured in DMEM supplemented with 10% FBS were resuspended in serum-free DMEM at 2×10^7 cells/mL immediately before transfection. Transfection of pCMV SPORT heart cell expression cDNA library was performed by electroporation (220 V, 960 μFD) at 50 μg of plasmid cDNA per mL. Forty-eight hours later, the transfected cells were stimulated with 1 mmol/L H_2O_2 for 16 hours in serum-free DMEM to induce cell death and cDNA was recovered from the survived colonies. This procedure was repeated 4 times.[1]

Received May 28, 2003; revision received August 4, 2003; accepted August 7, 2003.

From the Department of Cardiovascular Science and Medicine (Y.Z., W.Z., M.S., Y.Q., H.A., H.T., M.M., T.M., H.T., T.N., I.K.), Chiba University Graduate School of Medicine, Chiba; Department of Cardiovascular Medicine (N.T.), University of Tokyo Graduate School of Medicine, Tokyo; and Department of Bio-Signal Analysis, Applied Medical Engineering Science (A.N.), Yamaguchi University Graduate School of Medicine, Yamaguchi, Japan.

*These authors contributed equally to this study.

Correspondence to Issei Komuro, MD, PhD, Department of Cardiovascular Science and Medicine, Chiba University, Graduate School of Medicine, 1-8-1 Inohana, Chuo-ku, Chiba 260-8670, Japan. E-mail komuro-tky@umin.ac.jp

Circulation is available at http://www.circulationaha.org

DOI: 10.1161/01.CIR.0000101923.54751.77

Cell Preparation and DNA Transfection

Primary cultures of cardiomyocytes were prepared from ventricles of 1-day-old Wistar rats, and 0.5 to 10 μg of HSF1 cDNA per dish was transfected into COS7 cells with the 1.5 to 20 μg of green fluorescence protein (GFP)-expressing vector by the standard calcium phosphate method.[9,10]

ΔHSF1 Transgenic Mice and Murine Ischemia/Reperfusion Model

Construction of the ΔHSF1 transgene and generation of the ΔHSF1 transgenic mice have been previously described.[8] Ischemia/reperfusion injury was produced in 12-week-old male transgenic mice and their littermate wild-type mice by transiently ligating the left coronary artery.[11] All protocols were approved by the guidelines of Chiba University.

Gel Mobility Shift Assay

DNA binding activities of HSF1 was examined as previously described using a self-complementary consensus HSE oligonucleotide (5′-CTAGAAGCTTCTAGAAGCTTCTAG-3′) (Sigma) as a probe.[8]

Antisense Experiment

Phosphothionate antisense oligonucleotides (5′-CTAGAAGCTTCTAGAAGCTTCTAG-3′) of HSF1 or scramble oligonucleotides (5′-AGTCACGATCTATAGATCTGAGTC-3′) (Sigma) were prepared and applied to the culture medium (10 μmol/L) before the thermal preconditioning treatment of cardiomyocytes.

Apoptosis Analysis

Apoptotic death of cardiomyocytes was determined by TUNEL and by DNA ladder analysis, as previously described.[10,12]

Western Blot Analysis

Total protein extracts from the heart or immunoprecipitates were electrophoresed on an SDS-polyacrylamide gel (SDS-PSGE) and transferred to Immobilon-p membrane (Millipore). The blotted membranes were incubated with antibodies to HSF1, HSP27, *HSP70, HSP90, HSP110*, caspase3, Apaf1, Akt, phospho-Akt (Ser 473), Jun N-terminal kinase (JNK), phospho-JNK (Thr 183/Tyr 185), and α-actin (Santa Cruz Biotechnology), respectively. Immunoreactivity was detected using an enhanced chemiluminescence reaction system according to the manufacturer's instructions.

Statistics

Data are shown as mean±SE. Multiple group comparison was performed by one-way ANOVA followed by the Bonferroni procedure for comparison of means. A 2-tailed Student *t* test was used to compare transgenic with nontransgenic specimens under identical conditions. $P<0.05$ was considered statistically significant.

Results

Cloning of Cardioprotective Genes

COS7 cells were transfected with a heart cDNA library and then exposed to lethal dose of H_2O_2. Six cDNA clones were isolated from independent colonies of surviving cells, and 3 of them were identical to HSF1. To confirm the protective role of HSF1, we transfected the isolated HSF1 cDNA into COS7 cells. Overexpression of the HSF1 protected COS7 cells from H_2O_2-induced death (Figure 1A), whereas other cDNA, such as GFP, had no effect (data not shown).

To examine whether HSF1 protects cardiomyocytes against H_2O_2, cultured cardiomyocytes were exposed to H_2O_2 after thermal preconditioning at 42°C for 60 minutes followed by additional culture at 37°C for 24 hours. Electrophoretic mobility shift assay using HSF1 binding sequence revealed that the shifted band was enhanced after the thermal preconditioning (Figure 1B), indicating that HSF1 was activated in cultured cardiomyocytes by thermal preconditioning. Agarose gel electrophoresis showed that DNA ladder formation was observed in the cells treated with H_2O_2, whereas the DNA fragmentation was barely detectable in control cells and cells pretreated with thermal preconditioning (Figure 1C). The antisense oligonucleotides of HSF1 but not the scramble oligonucleotides abolished the protective effect of thermal

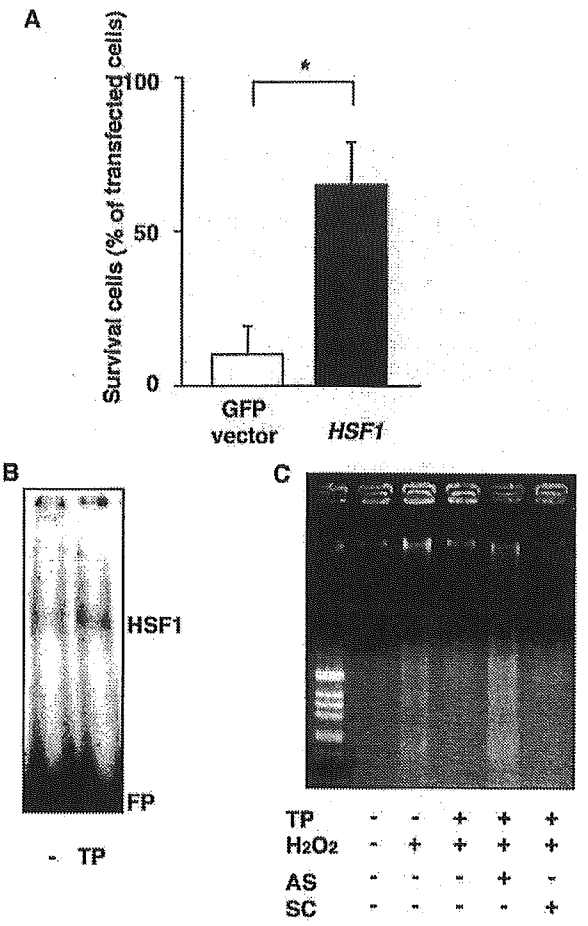

Figure 1. Protective effects of HSF1 in cultured cells. A, Survival of COS7 cells from H_2O_2 stress. COS7 cells were transfected with 2.5 μg of isolated *HSF1* cDNA with 7.5 μg of GFP expressing vector or GFP vector alone and additionally cultured with 1 mmol/L H_2O_2 after 24 hours. Survived cells are expressed as a percentage of transfected cells. Data are presented as mean±SE from 3 independent experiments. *$P<0.05$. B, DNA-binding activity of *HSF1*. Cultured cardiomyocytes were subjected to thermal preconditioning (TP) at 42°C for 60 minutes. A gel mobility shift assay was performed with whole-cell extracts using a DNA fragment containing HSE. A representative photograph from 3 independent experiments is shown. FP indicates free probe. C, DNA fragmentation. Cardiomyocytes with or without TP were exposed to 100 μmol/L H_2O_2 for 24 hours. Some cells were incubated with antisense (AS) or scrambled (SC) oligonucleotides of *HSF1* for 18 hours before TP. Genomic DNA was separated in 1.5% agarose gels and stained by ethidium bromide.

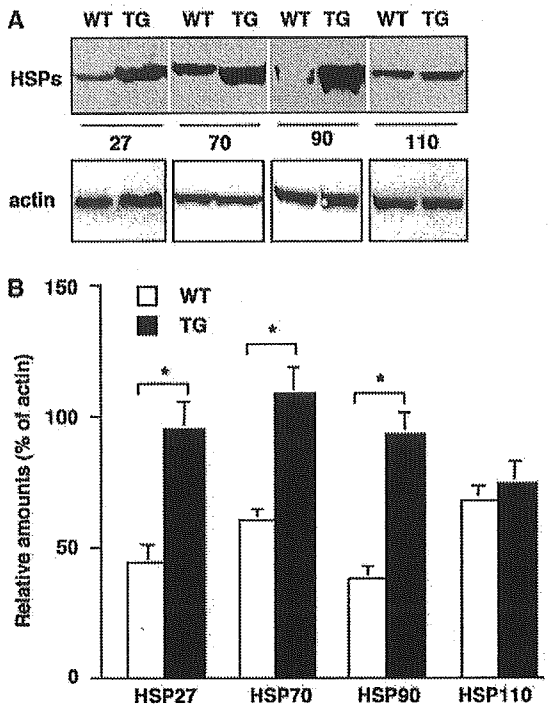

Figure 2. Expression of HSPs in the heart. A, Expression of HSPs levels in hearts from wild-type (WT) and transgenic (TG) mice were examined by Western blot analysis using each antibody. A representative photograph from 3 independent experiments is shown. α-actin blot was also presented as a loading control. B, Quantitative analysis of HSP protein expression. Intensities of HSPs and α-actin bands were measured by densitometric scanning of the autoradiograms. Relative amounts of HSPs are expressed as percentage of α-actin. Data are presented as mean±SE from 3 independent experiments. *$P<0.05$.

preconditioning (Figure 1C), suggesting that the thermal preconditioning protects cardiomyocytes from H_2O_2-induced cell death through activation of HSF1.

HSF1 Transgenic Mice

To elucidate the protective role of HSF1 in the heart, we examined the transgenic mice that overexpress Δ*HSF1*.[8] The transgenic mice were apparently healthy, and there were no significant differences in body weight, heart weight, blood pressure, and heart rate between the transgenic mice and littermate wild-type mice (data not shown).

Western blot analysis of heart extracts revealed that ΔHSF1 protein was expressed only in the adult transgenic mice, and there was no difference in expression levels of endogenous HSF1 between the transgenic and wild-type mice (data not shown).[8] The expression of HSPs 27, 70, and 90 was markedly upregulated in the transgenic heart compared with wild-type heart (Figures 2A and 2B).

Ischemia/Reperfusion Injury

Mice were subjected to cardiac ischemia for 40 minutes followed by reperfusion for 120 minutes. There were no abnormalities in ECG before ischemia in both the transgenic mice and wild-type mice (Figure 3). When the left coronary

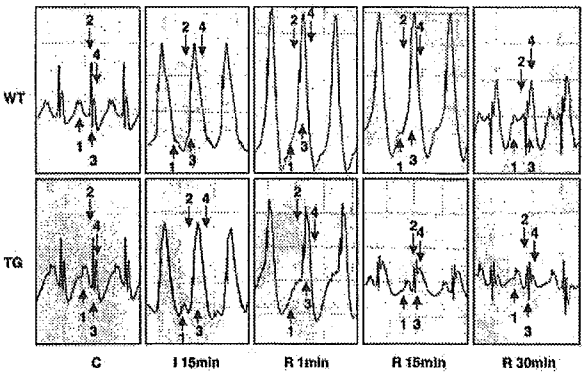

Figure 3. ECG recordings. ECG was recorded before and during ischemia/reperfusion. Representative ECG recordings before ischemia (C), at 15 minutes after ischemia (I 15min), and at 1, 15, and 30 minutes after reperfusion (R 1min, R 15min, and R 30min, respectively). Arrows 1 through 4 indicate P wave, QRS wave, ST segment, and T wave, respectively.

artery was occluded, the ST-segment was rapidly elevated in both types of mice. There was no significant difference in ECG change during ischemia between the transgenic and wild-type mice. When the suture was released to allow reperfusion, the ST-segment returned to baseline within 15 minutes in the transgenic mice whereas the ST-segment elevation remained elevated over 30 minutes in wild-type

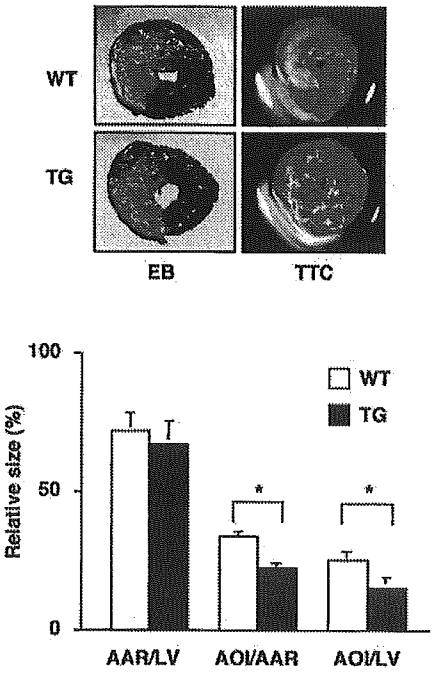

Figure 4. AAR and AOI. A, Representative photographs of wild-type (WT) and transgenic (TG) hearts stained by Evans blue dye (EB) and triphenyltetrazolium chloride (TTC) after ischemia/reperfusion (I/R). Red areas in left photographs indicate AAR, and pale white areas in right photographs indicate AOI. B, AAR is presented as a percentage of whole LV mass. AOI is expressed as a percentage of AAR and of whole LV mass. Values are mean±SE of 3 independent experiments. *$P<0.05$.

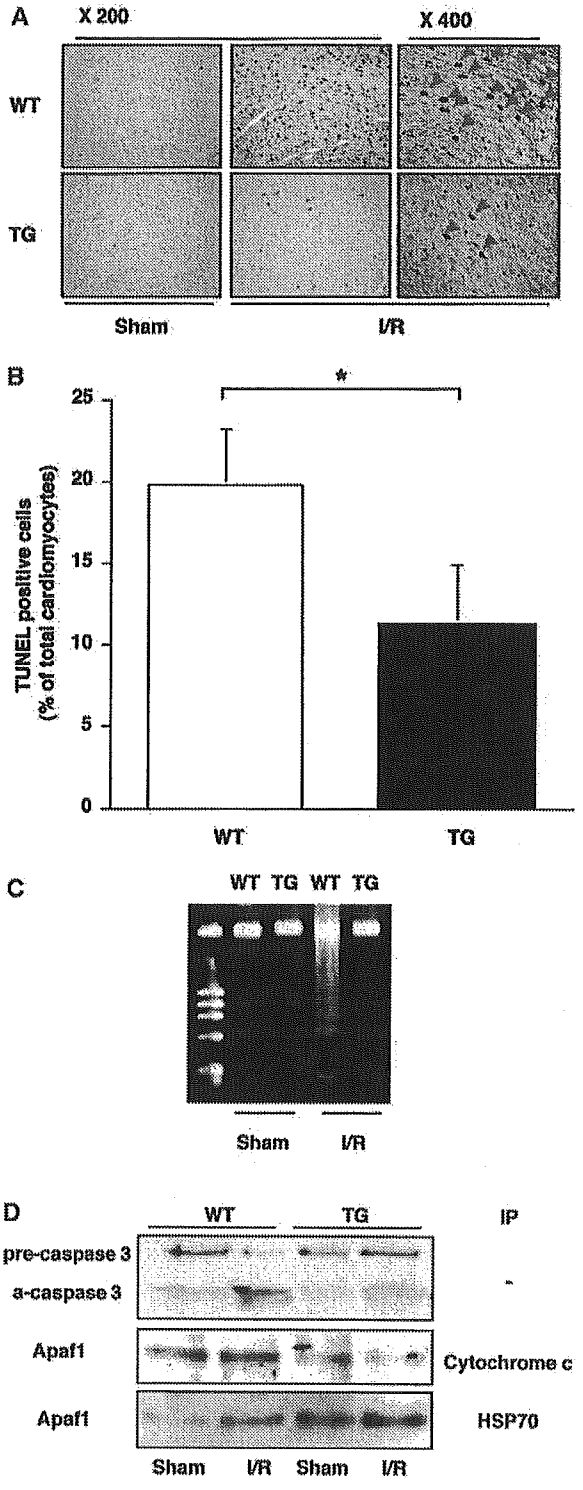

Figure 5. Apoptosis in the heart. A, TUNEL staining. Representative photographs in the edge of ischemic area after ischemia/reperfusion (I/R) or in similar area after sham operation (Sham) from wild-type (WT) and transgenic (TG) hearts are shown (original magnification ×200 and ×400). Arrows indicate TUNEL-positive cells. B, Numbers of TUNEL-positive cells. Fifty fields in ischemic area from 5 sections of each heart were counted. The number is expressed as percentage of total cardiomyocytes. *$P<0.05$. C, DNA ladders. Genomic DNA from the heart was separated in 1.5% agarose gels and stained by ethidium bromide. D, Activation of caspase 3 and Apaf1. WT and the TG mice were subjected to I/R. Total cell extracts from the heart or immune complexes with cytochrome C or HSP70 were subjected to SDS-PAGE. Western blot analysis was performed using antibodies against caspase 3 or Apaf1. Pre-caspase 3 indicates precursor of caspase 3; a-caspase 3, activated caspase 3; and IP, immunoprecipitation. Representative autoradiograms from 3 independent experiments are shown.

mice. These results suggest that Δ*HSF1* exerts its protective effect on the electrical activity of myocardium against ischemia/reperfusion injury.

We also measured areas at risk (AAR) and areas of infarction (AOI) after ischemia/reperfusion. Because we ligated the left coronary artery at the most proximal portion, the occlusion consistently created a large ischemic area (AAR, red myocardium in Figure 4A, left), and there was no difference in the ischemic area between both groups. However, there was a significant difference in infarct size (AOI, pale white areas in Figure 4A, right). Both areas of infarction/left ventricle (LV) and areas of infarction/ischemic area were significantly smaller in the transgenic group than those in the nontransgenic mice (Figure 4B).

Apoptosis in Mice

Ischemia/reperfusion injury has been reported to induce apoptosis in cardiomyocytes.[13] Apoptotic death of cardiomyocytes was examined in the heart by TUNEL and DNA ladder analysis. Ischemia/reperfusion induced apoptosis in many cardiomyocytes (Figures 5A and 5B) and produced marked DNA ladder formation (Figure 5C) in the ischemic area of wild-type heart. The number of apoptotic cells and the DNA fragmentation were significantly less in the Δ*HSF1* transgenic heart than the wild-type one (Figures 5A, 5B, and 5C). Caspase 3 was activated and Apaf1-cytochrome C complex was significantly increased in wild-type mice but less in the transgenic mice after ischemia/reperfusion (Figure 5D). Instead, more Apaf1-*HSP70* association was observed in the transgenic heart than in the wild-type heart after ischemia/reperfusion (Figure 5D).

Activation of Protein Kinases

It has been reported that many stresses, including ischemia/reperfusion, activate several protein kinases, including Akt/protein kinase B and JNK,[14] and that activation of Akt induces survival of cells whereas activation of JNK usually triggers death-signaling pathways. In the basal state, there was no difference in the activity of Akt and JNK between the wild-type and the transgenic heart (Figures 6A through 6C). Ischemia/reperfusion induced a significant activation of Akt and JNK in the wild-type heart (Figures 6A through 6C), suggesting that both survival and death signaling were activated in response to ischemia/reperfusion. In the transgenic heart, activation of Akt in response to ischemia/reperfusion was more prominent whereas activation of JNK was weaker than in the wild-type heart (Figures 6A through 6C). Although there was no change in protein

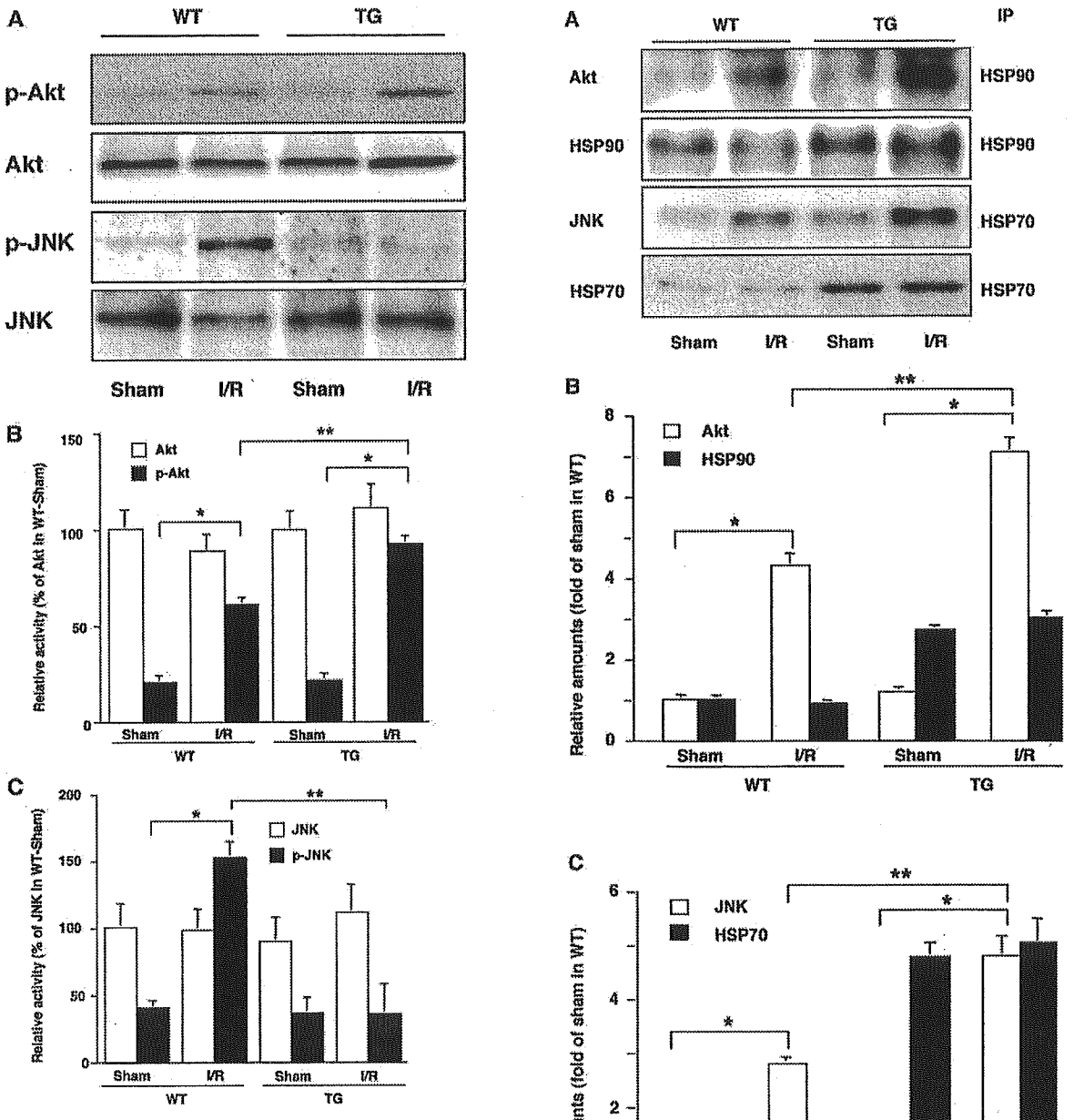

Figure 6. Activation of Akt and JNK in the heart. A, Protein extracts from the total heart were subjected to SDS-PAGE, and Western blot analysis was performed. p-Akt indicates phosphorylated Akt; p-JNK, phosphorylated JNK. B and C, Quantitative analysis of Akt (B) and JNK (C) activities. The intensities of Akt or p-Akt and JNK or p-JNK bands were measured by densitometric scanning of the autoradiograms. Relative amounts of Akt or p-Akt and JNK or p-JNK are expressed as percentage of Akt and JNK, respectively, in sham-operated wild-type (WT) mice. TG indicates transgenic mice; I/R, ischemia/reperfusion. Data are mean±SE from 3 independent experiments. *,**$P<0.05$.

levels of Akt and JNK after ischemia/reperfusion (Figure 6A), the amount of Akt and JNK that bound to *HSP90* and *HSP70*, respectively, was more markedly increased in the transgenic heart compared with the wild-type heart after ischemia/reperfusion (Figures 7A through 7C).

Figure 7. Association of Akt and JNK with HSPs. A, Protein extracts of the heart were immunoprecipitated (IP) using antibodies against HSP70 or HSP90. Immune complexes were subjected to SDS-PAGE, and the membranes were incubated with antibodies as indicated. B and C, Quantitative analysis of Akt (B) and JNK (C) bound to HSPs. Intensities of Akt, JNK, and HSP bands were measured by densitometric scanning of the autoradiograms. Relative amounts of Akt, JNK, and HSP are expressed as fold of Akt, JNK, and HSPs, respectively, in sham-operated wild-type (WT) or transgenic (TG) mice. I/R indicates ischemia/reperfusion. Data are mean±SE from 3 independent experiments. *,**$P<0.05$.

Discussion

The functional cloning system, death trap, is designed to isolate molecules that protect cells from death.[1] Using this method, *HSF1* gene was isolated from heart cDNA library. *HSF1*, a major heat stress-responding factor, upregulates many *HSP* genes, including *HSP110*, *HSP90*, *HSP70*, and small *HSPs*.[2,3] Expression levels of *HSP90*, *HSP70*, and *HSP27* were significantly elevated in the heart of transgenic mice overexpressing Δ*HSF1* compared with wild-type mice. Although *HSP70* has been reported to have a cardioprotective function,[15–17] the role of other HSPs in the heart is largely unknown. The Δ*HSF1* transgenic mouse provides a good model to examine the role of activated *HSF1* and of multiple HSPs in the heart.

Hearts of the transgenic mice were more resistant to ischemia/reperfusion injury, as indicated by faster recovery of ST-segment elevation in ECG and smaller infarct size. There are several potential mechanisms underlying the cardioprotective effect of HSPs.[4,5] HSPs are generally believed to help the correct folding of many proteins and restore their functional structures or target denatured proteins to the lysosome for degradation as molecular chaperones.[4,5] These functions of HSPs as molecular chaperones play important roles in maintaining the normal cell functions and promoting cell survival. Functions of HSPs other than molecular chaperones have recently attracted much attention in many organs, including the heart. It has been reported that accumulation of HSPs in myocardium shows an ATP-sparing effect that enhances preservation of high-energy phosphates.[4,5] Repeated coronary occlusions, called ischemic preconditioning, have been reported to induce rapid normalization of the elevated ST-segment during reperfusion by improving regional acidosis and hypokalemia.[18] HSPs may be involved in the faster normalization of ST-segment after reperfusion through restoration of the metabolic and ionic balance.

We showed here that ischemia/reperfusion induced less apoptosis of cardiomyocytes in the Δ*HSF1* transgenic mice than wild-type mice. Apoptosis is induced by defined biochemical mechanisms, including release of cytochrome C from mitochondria to cytoplasm and activation of Apaf1 through forming an apoptosome complex.[19,20] The apoptosome complexes cleave and activate caspase 3, leading to the inevitable fate of cell death. It has been reported that overexpression of caspase 3 in the heart significantly increases infarct size[21] and that the treatment with a caspase inhibitor conversely reduces infarct size.[22] HSPs have been reported to inhibit the formation of the apoptosome complexes through forming cytosolic complexes with Apaf1 or cytochrome C and then inhibit activation of caspases.[19,20] In this study, Apaf1 formed more complexes with *HSP70* and less with cytochrome C in the transgenic heart than the wild-type one, and ischemia/reperfusion activated Apaf1 and caspase 3 more weakly in the transgenic heart than the wild-type one. These results and observations suggest that HSPs protect cardiomyocytes from ischemia/reperfusion-induced cell death at least in part through forming complexes with Apaf1 and inhibiting the activation of caspase 3.

Both Akt and JNK were activated in the heart after ischemia/reperfusion, as reported previously.[23,24] Activation of Akt has been reported to protect cardiomyocytes against various stresses, such as oxidative stress[25] and the ischemia/reperfusion injury,[26] whereas JNK has been indicated to induce apoptosis during ischemia/reoxygenation in rat cardiomyocytes.[27] In the present study, ischemia/reperfusion activated more Akt and less JNK in the transgenic heart than the wild-type one. HSP90 has been reported to bind to Akt and promote activation of Akt through inhibition of protein phosphatase 2A.[28] Another recent report also showed that overexpression of *HSP90* leads to an increased phosphorylation of Akt.[29] On the other hand, Hsp70 family can suppress stress-activated signaling by directly binding to JNK.[14,30] We here observed that association between both *HSP90* and Akt and *HSP70* and JNK was more enhanced in the *HSF1* transgenic heart than in the wild-type heart. These results collectively suggest that HSPs exert cardioprotective effects through activation of Akt and suppression of JNK. Additional study is needed to elucidate which mechanism plays a major role in *HSF1*/HSP-induced protection of cardiomyocytes.

Acknowledgments

This work was supported by a Grant-in-Aid for Scientific Research, Developmental Scientific Research, and Scientific Research on Priority Areas from the Ministry of Education, Science, Sports, and Culture and by a grant for research on life science from Uehara Memorial Foundation, Japan (to I. Komuro).

References

1. Vito P, Lacana E, D'Adamio L. Interfering with apoptosis: Ca^{2+}-binding protein ALG-2 and Alzheimer's disease gene ALG-3. *Science.* 1996;271: 521–525.
2. Benjamin IJ, McMillan DR. Stress (heat shock) proteins: molecular chaperones in cardiovascular biology and disease. *Circ Res.* 1998;83: 117–132.
3. Pirkkala L, Nykanen P, Sistonen L. Roles of the heat shock transcription factors in regulation of the heat shock response and beyond. *FASEB J.* 2001;15:1118–1131.
4. Gray CC, Amrani M, Yacoub MH. Heat stress proteins and myocardial protection: experimental model or potential clinical tool? *Int J Biochem Cell Biol.* 1999;31:559–573.
5. Latchman DS. Heat shock proteins and cardiac protection. *Cardiovasc Res.* 2001;51:637–646.
6. Pockley AG. Heat shock proteins, inflammation, and cardiovascular disease. *Circulation.* 2002;105:1012–1017.
7. Knowlton AA, Sun L. Heat-shock factor-1, steroid hormones, and regulation of heat-shock protein expression in the heart. *Am J Physiol Heart Circ Physiol.* 2001;280:H455–H464.
8. Nakai A, Suzuki M, Tanabe M. Arrest of spermatogenesis in mice expressing an active heat shock transcription factor 1. *EMBO J.* 2000; 19:1545–1554.
9. Zou Y, Komuro I, Yamazaki T, et al. Cell type-specific angiotensin II-evoked signal transduction pathways: critical roles of Gbetagamma subunit, Src family, and Ras in cardiac fibroblasts. *Circ Res.* 1998;82: 337–345.
10. Zhu W, Shiojima I, Hiroi Y, et al. Functional analyses of three Csx/Nkx-2.5 mutations that cause human congenital heart disease. *J Biol Chem.* 2000;275:35291–35296.
11. Harada K, Komuro I, Hayashi D, et al. Angiotensin II type 1a receptor is involved in the occurrence of reperfusion arrhythmias. *Circulation.* 1998; 97:315–317.
12. Gu Y, Zou Y, Aikawa R, et al. Growth hormone signalling and apoptosis in neonatal rat cardiomyocytes. *Mol Cell Biochem.* 2001;223:35–46.
13. Fliss H, Gattinger D. Apoptosis in ischemic and reperfused rat myocardium. *Circ Res.* 1996;79:949–956.
14. Gabai VL, Sherman MY. Interplay between molecular chaperones and signaling pathways in survival of heat shock. *J Appl Physiol.* 2002;92: 1743–1748.

15. Plumier JC, Ross BM, Currie RW, et al. Transgenic mice expressing the human heat shock protein 70 have improved post-ischemic myocardial recovery. *J Clin Invest.* 1995;95:1854–1860.
16. Marber MS, Mestril R, Chi SH, et al. Overexpression of the rat inducible 70-kD heat stress protein in a transgenic mouse increases the resistance of the heart to ischemic injury. *J Clin Invest.* 1995;95:1446–1456.
17. Radford NB, Fina M, Benjamin IJ, et al. Cardioprotective effects of 70-kDa heat shock protein in transgenic mice. *Proc Natl Acad Sci U S A.* 1996;93:2339–2342.
18. Figueras J, Segura R, Bermejo B. Repeated 15-minute coronary occlusions in pigs increase occlusion arrhythmias but decrease reperfusion arrhythmias that are associated with extracellular hypokalemia. *J Am Coll Cardiol.* 1996;28:1589–1597.
19. Saleh A, Srinivasula SM, Balkir L, et al. Negative regulation of the Apaf-1 apoptosome by Hsp70. *Nat Cell Biol.* 2000;2:476–483.
20. Pandey P, Saleh A, Nakazawa A, et al. Negative regulation of cytochrome c-mediated oligomerization of Apaf-1 and activation of procaspase-9 by heat shock protein 90. *EMBO J.* 2000;19:4310–4322.
21. Condorelli G, Roncarati R, Ross JJ, et al. Heart-targeted overexpression of caspase3 in mice increases infarct size and depresses cardiac function. *Proc Natl Acad Sci U S A.* 2001;98:9977–9982.
22. Okamura T, Miura T, Takemura G, et al. Effect of caspase inhibitors on myocardial infarct size and myocyte DNA fragmentation in the ischemia-reperfused rat heart. *Cardiovasc Res.* 2000;45:642–650.
23. Mockridge JW, Marber MS, Heads RJ. Activation of Akt during simulated ischemia/reperfusion in cardiac myocytes. *Biochem Biophys Res Commun.* 2000;270:947–952.
24. He H, Li HL, Lin A, et al. Activation of the JNK pathway is important for cardiomyocyte death in response to simulated ischemia. *Cell Death Differ.* 1999;6:987–991.
25. Pham FH, Sugden PH, Clerk A. Regulation of protein kinase B and 4E-BP1 by oxidative stress in cardiac myocytes. *Circ Res.* 2000;86:1252–1258.
26. Matsui T, Tao J, del MF, et al. Akt activation preserves cardiac function and prevents injury after transient cardiac ischemia in vivo. *Circulation.* 2001;104:330–335.
27. Hreniuk D, Garay M, Gaarde W, et al. Inhibition of c-Jun N-terminal kinase 1, but not c-Jun N-terminal kinase 2, suppresses apoptosis induced by ischemia/reoxygenation in rat cardiac myocytes. *Mol Pharmacol.* 2001;59:867–874.
28. Sato S, Fujita N, Tsuruo T. Modulation of Akt kinase activity by binding to Hsp90. *Proc Natl Acad Sci U S A.* 2000;97:10832–10837.
29. Brouet A, Sonveaux P, Dessy C, et al. Hsp90 and caveolin are key targets for the proangiogenic nitric oxide-mediated effects of statins. *Circ Res.* 2001;89:866–873.
30. Park HS, Lee JS, Huh SH, et al. Hsp72 functions as a natural inhibitory protein of c-Jun N-terminal kinase. *EMBO J.* 2001;20:446–456.

ACADEMIC PRESS

Available online at www.sciencedirect.com

SCIENCE DIRECT®

Experimental Cell Research 291 (2003) 56–69

Experimental Cell Research

www.elsevier.com/locate/yexcr

Early stage-specific inhibitions of cardiomyocyte differentiation and expression of Csx/Nkx-2.5 and GATA-4 by phosphatidylinositol 3-kinase inhibitor LY294002

Atsuhiko T. Naito,[a,1] Aki Tominaga,[a] Masahito Oyamada,[a,*] Yumiko Oyamada,[a] Isao Shiraishi,[b] Koshiro Monzen,[c] Issei Komuro,[d] and Tetsuro Takamatsu[a]

[a] *Department of Pathology and Cell Regulation, Kyoto Prefectural University of Medicine, Kyoto, Japan*
[b] *Division of Pediatrics, Children's Research Hospital, Kyoto Prefectural University of Medicine, Kyoto, Japan*
[c] *Department of Cardiovascular Medicine, University of Tokyo Graduate School of Medicine, Tokyo, Japan*
[d] *Department of Cardiovascular Science and Medicine, Chiba University Graduate School of Medicine, Chiba, Japan*

Received 4 March 2003, revised version received 23 June 2003

Abstract

Inhibition of phosphatidylinositol 3-kinase (PI3-kinase) has been reported to block cardiomyocyte differentiation. However, at which stage PI3-kinase plays this important role and what its molecular targets are remain unknown. To answer these questions, we induced cardiomyocyte differentiation of P19CL6 mouse embryonal carcinoma cells and investigated the activation of PI3-kinase by analyzing phospho-Akt. We also treated P19CL6 cells with the PI3-kinase-specific inhibitor LY294002 either continuously or at various time points and monitored the expression of cardiac contractile proteins and transcription factors. Most cells differentiated into sarcomeric myosin heavy chain (MHC)-positive cardiomyocytes on day 16 after induction. An increase in phospho-Akt was observed after induction and was maintained throughout the differentiation. LY294002 treatment restricted to the phase from days 0 to 4 was sufficient to inhibit cardiomyocyte differentiation in a dose-dependent manner. In contrast, LY294002 treatment either from days 4 to 8 or from days 8 to 12 did not cause significant changes in sarcomeric MHC expression. LY294002 treatment from days 0 to 4 also suppressed Csx/Nkx-2.5 and GATA-4 expression. These results demonstrate that PI3-kinase becomes activated and plays a pivotal role at a very early stage of cardiomyocyte differentiation, possibly by modulating the expression of the cardiac transcription factors.

Keywords: Phosphatidylinositol 3-kinase; Cardiomyocyte differentiation; LY294002; Csx/Nkx-2.5; GATA-4; P19CL6 cells; Akt

Introduction

[1]Early cardiomyocyte differentiation is divided into three stages, i.e., the precardioblast stage, cardioblast stage, and cardiomyocyte stage [1]. Cardiac lineage commitment occurs between the first and second stages upon induction of cardiac transcription factors such as Csx/Nkx-2.5 and GATA-4, but without cardiac contractile protein expression. Csx/Nkx-2.5 and GATA-4 are the earliest genes to be expressed in the cardiac field [2,3] and, after induction, and they form a transcriptional loop and up-regulate the expression of each other. Next, proliferation and differentiation of cardioblasts take place between the second and third stages, which are characterized by the expression of cardiac contractile protein genes such as myosin heavy chain (MHC) and myosin light chain (MLC) genes. Finally, maturation and maintenance of cardiomyocytes are observed after the third stage. Such processes of early cardiomyocyte differentiation are induced and maintained by autocrine and paracrine secretion of several peptide factors including bone morphogenetic proteins (BMP) [4] and fibroblast growth

* Corresponding author. Department of Pathology and Cell Regulation, Kyoto Prefectural University of Medicine, Kawaramachi Hirokoji, Kamigyo-ku, Kyoto 602-8566, Japan. Fax: +81-75-251-5353.
E-mail address: oyamada@basic.kpu-m.ac.jp (M. Oyamada).
[1] Present address: Department of Cardiovascular Science and Medicine, Chiba University Graduate School of Medicine, Chiba, Japan.

0014-4827/$ – see front matter © 2003 Elsevier Inc. All rights reserved.
doi:10.1016/S0014-4827(03)00378-1

factors (FGF) [5]. However, very little is known about the precise molecular pathways by which these peptide factors effect signal transduction into the nucleus and coordinate cardiomyocyte differentiation.

Class IA and IB phosphatidylinositol 3-kinases (PI3-kinase) lie downstream of many receptor tyrosine kinases and G-protein-coupled receptors, respectively, and they phosphorylate phosphatidylinositol at the D-3 position of the inositol ring [6–8]. The resulting product, phosphatidylinositol-3,4,5-trisphosphate, activates various downstream proteins including a serine/threonine kinase Akt that possesses D-3 phosphorylated phosphoinositide-specific binding domains. Through these downstream proteins, PI3-kinase plays an essential role in a wide variety of cellular processes including intracellular trafficking, organization of the cytoskeleton, cell proliferation, and prevention of apoptosis [9]. PI3-kinase has also been suggested to play a role in differentiation of several cell lineages including skeletal myocytes [10–12], adipocytes [13,14], and erythroleukemia cells [15], which like cardiomyocytes are derived from mesodermal cells.

While much information has been gathered on the role of PI3-kinase in apoptosis, cell survival [16], and determination of the cell size of cardiomyocytes [17], little is known about the role of PI3-kinase in cardiomyocyte differentiation. Recently, it has been reported that the PI3-kinase inhibitor LY294002 blocked cardiomyocyte differentiation of embryonic stem (ES) cells [18] and down-regulated intracellular reactive oxygen species [19]. However, the stage at which PI3-kinase plays an important role in cardiomyocyte differentiation and what its molecular targets are remain unknown, because the ES cells in the cardiomyocyte differentiation system possess multipotency and low efficiency of differentiation into cardiomyocytes.

In contrast, in an in vitro culture system P19CL6 cells [20–23], a clonal derivative of P19 embryonal carcinoma cells [24], efficiently differentiate into beating cardiomyocytes under adherent conditions when treated with 1% dimethyl sulfoxide (DMSO) and do not differentiate into cells of other mesodermal lineage such as skeletal myocytes [20]. The in vitro differentiation of P19CL6 cells follows the normal developmental program of the cardiomyocyte in vivo. For example, it has been reported that P19CL6-cell-derived cardiomyocytes express cardiac transcription factors such as Csx/Nkx-2.5 and GATA-4, followed by the expression of cardiac contractile proteins such as cardiac isoforms of MHC and MLC [21,22]. Therefore, this culture system offers great advantages for the investigation of the molecular events that occur at each stage of the cardiomyocyte differentiation, i.e., the precardioblast stage, cardioblast stage, and cardiomyocyte stage.

In the present study, we hypothesized that the PI3-kinase-mediated pathway regulates cardiomyocyte differentiation at specific periods and that this regulation involves the modulation of expression of cardiac transcription factors such as Csx/Nkx-2.5 and GATA-4. To test these hypotheses, we treated P19CL6 cells with a specific inhibitor of PI3-kinase, LY294002, either continuously or at various time points, and monitored the appearance of spontaneously beating cardiomyocytes and the expression of cardiac contractile proteins and transcription factors. We also investigated the activation of the PI3-kinase during cardiomyocyte differentiation of P19CL6 cells by analyzing phosphorylation of Akt and studied its relation to the expression of cardiac transcription factors, Csx/Nkx-2.5 and GATA-4.

Materials and methods

Materials

LY294002 and wortmannin were purchased from BioMol Research Laboratories (Plymouth Meeting, PA). A monoclonal antibody against sarcomeric MHC (clone MF20) developed by Dr. Fischman was obtained from the Developmental Studies Hybridoma Bank maintained at the University of Iowa, Department of Biological Sciences. Anti-Akt and anti-phospho-Akt (Ser473) antibodies were purchased from Cell Signaling Technology (Beverly, MA).

Cell culture

P19CL6 cells were cultured essentially as described previously [20–22] with a slight modification. In brief, the cells were grown in 100-mm tissue culture dishes under adherent conditions with α-minimum essential medium (Invitrogen, Tokyo, Japan) supplemented with 10% fetal bovine serum (Invitrogen), penicillin (100 U/ml), and streptomycin (100 mg/ml) (growth medium) and maintained in a 5% CO_2 atmosphere at 37°C. To induce cardiomyocyte differentiation under adherent conditions, P19CL6 cells were plated at a density of 3.7×10^5 in a 60-mm tissue culture dish in the growth medium. Twelve hours later, the medium was replaced with growth medium containing 1% DMSO (Sigma, Tokyo, Japan) (differentiation medium). The medium was changed every 2 days. The days of differentiation are numbered consecutively beginning after the first day of the DMSO treatment (day 0).

Reverse transcription polymerase chain reaction (RT-PCR)

Differentiation-induced P19CL6 cells were harvested and stored at −80°C until RNA extraction. RNA extraction was performed using RNeasy mini kit (Qiagen, Tokyo, Japan). In order to exclude the contamination of genomic DNA, extracted RNA was treated with DNase by using RNase-Free DNase Set (Qiagen). An equal amount of total RNA (1 μg) was used for first-strand cDNA synthesis using oligo-dT primer and 0.25 U/μl avian myeloblastosis virus reverse transcriptase XL (Takara, Otsu, Japan) in a reaction volume of 20 μl according to the manufacturer's instruc-

tions. For semiquantitative analysis, reverse transcribed products were pooled and fourfold serial dilutions were used for PCR. PCR was performed in a reaction volume of 20 μl with 200 nM deoxynucleoside triphosphates, 500 nM each of sense and antisense primers, and 2.5 U/100 μl *Taq* polymerase (Takara). The amplification reaction was carried out in a Gene Amp PCR System 2400 (Applied Biosystems, Tokyo, Japan). Primer sequences were used as described in previous reports [21,25,26]. PCR was performed for 1 cycle at 94°C for 5 min, followed by 25–35 cycles of denaturation at 94°C for 30 s, annealing at 56–64°C, depending on the melting temperature of the primer sequence, for 30 s, and extension at 72°C for 1 min. Every PCR condition was confirmed to be within the linear range and within the semiquantitative range for these specific genes and primer pairs. To confirm that the obtained bands were not derived from contaminated genomic DNA, a negative experiment was done for each sample without reverse transcriptase before PCR. Amplified samples were electrophoresed on 2% agarose gels and stained with ethidium bromide. For semiquantitative RT-PCR analysis, PCR was carried out on undiluted cDNA and on fourfold serial dilutions of cDNA, and the intensities of the ethidium-bromide-stained bands for Csx/Nkx-2.5 and GATA-4 were quantified using NIH Image (Wayne Rasband; NIH) and subsequently normalized to β-actin mRNA levels. The relative expression levels in different samples were determined by calculating the fold dilution of the undiluted positive control cDNA which would be required for similar signal intensities. The data are expressed as percentages for Csx/Nkx-2.5 and GATA-4 expression in LY294002-treated cells compared to that of the positive control.

Western blotting

Cells grown on culture dishes were washed twice with ice-cold phosphate-buffered saline (PBS) and then directly lysed in 2x sodium dodecyl sulfate (SDS) gel loading buffer (125 mM Tris–HCl, pH 6.8, 4% SDS, 20% glycerol, and 1 mM phenylmethylsulfonyl fluoride) containing a mixture of phosphatase inhibitors, 10 mM sodium fluoride, 1 mM sodium orthovanadate, and 10 mM sodium pyrophosphate. The lysates were sonicated with a sonicator (Microson Model No. XL2000; Misonix, Inc., Farmingdale, NY) at setting 2 for 30 s on ice and centrifuged at 15,000*g* for 10 min at 4°C, and the supernatants were then carefully removed and stored at −80°C until use. Protein concentration was determined by using the BCA Protein Assay kit (Pierce, Rockford, IL). Proteins (40 μg) were subjected to 10% SDS polyacrylamide gel electrophoresis and subsequently transferred onto Hybond ECL membranes (Amersham, Piscataway, NJ) using semidry blotting. Membranes were stained with Ponceau S Solution (Sigma) and photographed to confirm equal loading of the protein samples. After being washed with Tris-buffered saline (pH 7.6) containing 0.1% Tween 20 (TBS-T), membranes were incubated for 1 h at room temperature in blocking buffer (5% skim milk in TBS-T) and then reacted with anti-Akt or anti-phospho-Akt (Ser473) antibodies (1:500 dilution) overnight at 4°C. After washes with TBS-T, membranes were reacted with horseradish-peroxidase-conjugated anti-rabbit antibody (1:2,000 dilution) for 1 h at room temperature. After washes with TBS-T, detection was performed using ECL Western blotting detection reagents (Amersham) and Hyperfilm ECL (Amersham).

Immunofluorescence

Cells were washed with PBS and then fixed with ethanol at −20°C for 10 min. After incubation in PBS supplemented with 5% skim milk for 30 min at room temperature to block nonspecific labeling, a monoclonal antibody against sarcomeric MHC (MF20; 1:50 dilution) was applied overnight at 4°C. After three 5-min washes with PBS, incubation with Alexa-488-labeled goat anti-mouse IgG (1:500 dilution; Molecular Probes, Eugene, OR) was performed for 1 h at room temperature. After final rinses in PBS, the cells were counterstained with propidium iodide (PI) and mounted in Vectorshield (Vector Laboratories, Burlingame, CA). All solutions for antibody dilutions were made in PBS containing 1% bovine serum albumin, 0.1% sodium azide, and 0.1% Triton X-100. The cells were viewed and photographed with a confocal laser scanning microscope (Olympus Fluoview system; Olympus, Tokyo, Japan) coupled to an inverted microscope (IX70; Olympus).

For morphometric analysis for the expression of sarcomeric MHC stained with MF20, all aspects of cell processing, immunostaining, and imaging were rigorously standardized. To exclude the possibility that variations in immunostaining on different dates affected the morphometric data, cells were immunostained and analyzed at the same time. Digital images were obtained from randomly selected fields using the 10X objective lens and a zoom setting of 1 under the same conditions, i.e., laser power = 35 mW, pinhole size = 100 μm, ND filter = 50%, photomultiplier voltage = 720 V, and scanning speed = 7.8 s/frame. The images were transferred to a Macintosh computer, converted into 8-bit images (256 levels), and analyzed using the NIH Image program (Wayne Rasband; NIH). A binary overlay was created automatically by a set threshold of 30 on the 255-point grayscale to eliminate the background cell outlines. Then the binary overlaid area in the area of interest was analyzed. Data are expressed as means ± SD MF20-positive area (pixel × pixel) calculated as a percentage of that for control P19CL6 cells cultured in differentiation medium without PI3-kinase inhibitors. At least four different fields were measured for each dish. We confirmed that on day 16, when cells were immunostained using MF20, the cells were confluent and no cell-free spaces were present in the images under any of the different conditions employed in this study.

To examine the effect of LY294002 on cell proliferation,

we monitored the DNA replication by bromodeoxyuridine (BrdU) labeling. Cells were incubated with fresh medium containing 20 μM BrdU (Sigma) at 37°C for 15 min. Cells were fixed in 2% paraformaldehyde at room temperature for 10 min, washed in PBS, incubated in methanol at −20°C for 15 min, and treated with 2 N HCl for 1 h. The cells were incubated with a sheep anti-BrdU polyclonal antibody (1:500 dilution; Molecular Probes) and then with Alexa 488 donkey anti-sheep IgG (1:500 dilution; Molecular Probes). All nuclei were counterstained with PI.

To determine the effect of LY294002 on apoptosis, we carried out terminal deoxynucleotidytransferase-mediated dUTP-biotin nick-end labeling (TUNEL) assay according to the manufacturer's instructions (ApotDETEK; Enzo Diagnostics, Farmingdale, NY) with a slight modification. Instead of fixation with acetone, cells were fixed in 2% paraformaldehyde on ice for 15 min, washed twice in PBS, and then incubated in ice-cold 70% ethanol for at least 1 h. TUNEL was detected using Alexa-488-labeled streptavidin (1:1000 dilution; Molecular Probes). All nuclei were counterstained with PI.

Statistics

Data are expressed as the mean ± SD from multiple experiments. Statistical analysis was performed using the StatView version 5.0 (SAS Institute, Cary, NC). Differences between control values and experimental values were determined by ANOVA, Dunnett's test, the Tukey–Kramer test, and the Mann–Whitney U test. Significant differences were defined as $P < 0.05$.

All results shown here were confirmed by at least two different series of experiments.

Results

In vitro cardiomyocyte differentiation of P19CL6 cells

Twelve hours after P19CL6 cells were plated on 60-mm dishes at a density of 3.7×10^5, when the cells were completely attached to the bottom of the dish, the medium was replaced with differentiation medium containing 1% DMSO (Fig. 1A). On day 4 (4 days after the initiation of DMSO treatment), cells had reached confluence, but they continued to proliferate and formed embryoid-body-like aggregates and multilayer sheets through day 8. After day 8, proliferation of the cells ceased and some cells showed spontaneous contraction. The area of contracting cells expanded multifocally thereafter and reached a plateau around day 12. On day 16, more than 80% of the cells had differentiated into synchronously contracting cardiomyocytes which were positive for the anti-sarcomeric MHC antibody, MF20 (Fig. 1B). At higher magnification, cross striations were demonstrated with MF20 immunolabeling (Fig. 1B, inset). The expressions of cardiac-specific genes including cardiac transcription factors and cardiac contractile protein genes were analyzed by RT-PCR on days 4, 8, and 12 of differentiation (Fig. 1E). Cardiac transcription factors, Csx/Nkx-2.5 and GATA-4, were expressed from day 4 and up-regulated through day 12. Cardiac α-MHC and a ventricular isoform of MLC (MLC-2v) were expressed from day 8, and the gene expression increased on day 12. These results indicate that the P19CL6 in vitro differentiation system fosters the differentiation program resulting in contracting cardiomyocytes in a manner that parallels the sequence of events occurring in the mouse embryo. In contrast, when P19CL6 cells were cultured in growth medium that did not contain DMSO, cells grew well but did not differentiate into cardiomyocytes (data not shown), consistent with the reported results [20–22].

Blocking of cardiomyocyte differentiation by PI3-kinase inhibitors

To examine whether PI3-kinase plays a role in cardiomyocyte differentiation, P19CL6 cells were treated with differentiation medium containing LY294002 (20 μM), a specific, aqueous stable inhibitor of PI3-kinase [27], throughout the differentiation process (Fig. 2A). Differentiation into cardiomyocytes was analyzed by RT-PCR for cardiac contractile protein genes on day 12 and by immunostaining using MF20 on day 16. We found that, in the presence of LY294002, no P19CL6 cells differentiated into beating cardiomyocytes. No MF20-positive area was observed in the cells treated with LY294002 at 20 μM (Fig. 2C and F), although the cells reached confluence (Fig. 2D). Inhibitory effects of PI3-kinase inhibitors on cardiomyocyte differentiation were further confirmed by using wortmannin, another PI3-kinase inhibitor which is structurally dis-

Fig. 1. Cardiomyocyte differentiation of P19CL6 cells. Schematic diagram of the experiment (A). P19CL6 cells were plated at a density of 3.7×10^5 in a 60-mm tissue culture dish in the growth medium. Twelve hours later, medium was replaced with growth medium containing 1% DMSO (differentiation medium). The medium was changed every 2 days. Days of differentiation are numbered consecutively beginning after the first day of the DMSO treatment (day 0). On day 16 (B), cells were stained for anti-sarcomeric MHC antibody (MF20). Note that most P19CL6 cells have differentiated into sarcomeric MHC-positive cardiomyocytes. Inset: Higher magnification reveals cross striations. Scale bar, 2 μm. Nuclear staining with propidium iodide (PI) (C). Phase-contrast photomicrograph (D). B, C, and D were taken from the same field. Scale bars, 50 μm. Expression of β-actin, Csx/Nkx-2.5, GATA-4, α-MHC, and MLC-2v on days 0, 4, 8, and 12 (E) was analyzed by RT-PCR for cells that were cultured in the growth medium alone (−DMSO) and for cells cultured in the differentiation medium (+DMSO). RNA (1 μg) was reverse transcribed, and PCR was performed using gene-specific primers. The gene products were analyzed by agarose gel electrophoresis and stained with ethidium bromide. M, molecular weight marker (ϕX174/*Hae* III). Expression of β-actin is shown as an internal control.

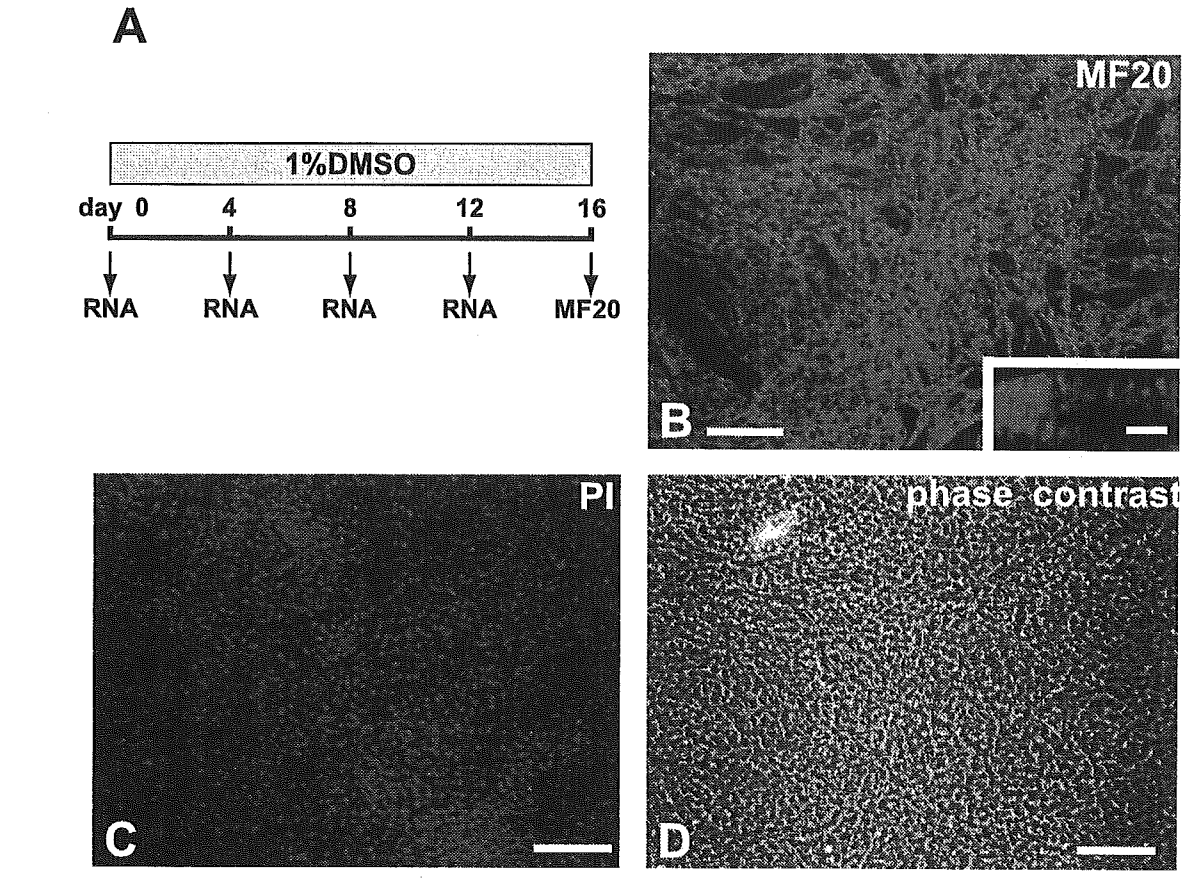
A
1%DMSO
day 0
4
8
12
16
RNA
RNA
RNA
RNA
MF20
MF20
B
PI
C
phase contrast
D

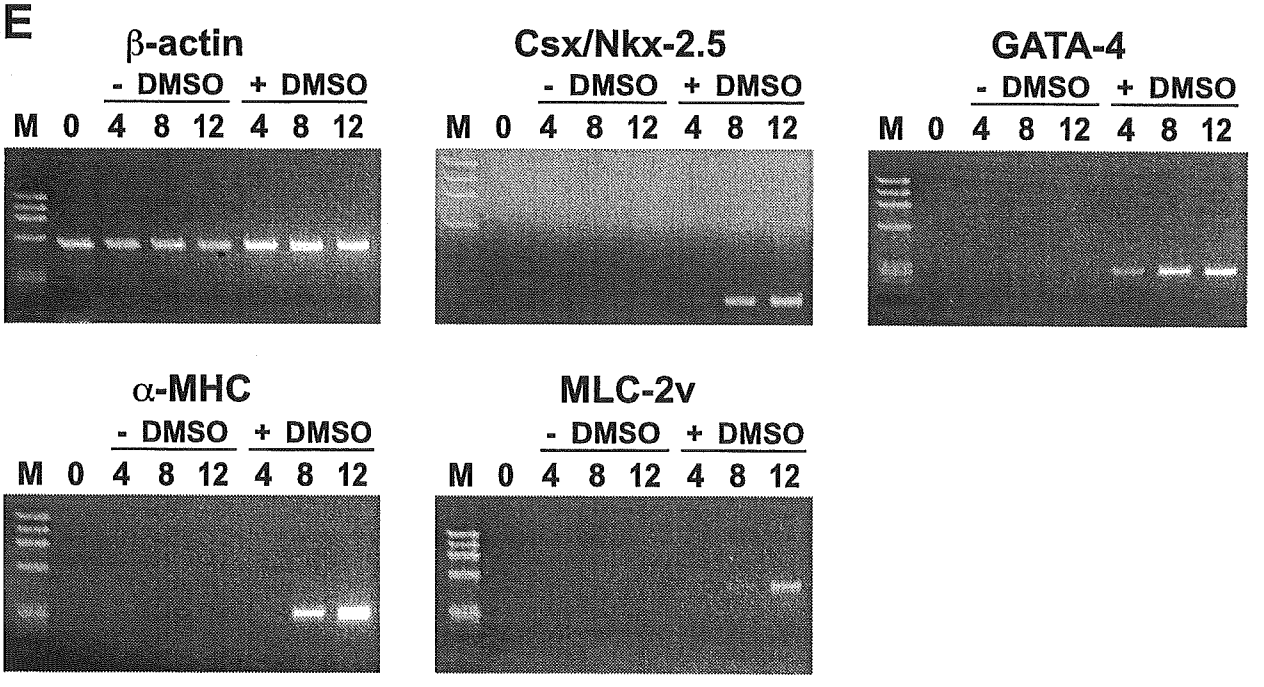
E
β-actin
- DMSO
+ DMSO
M 0 4 8 12 4 8 12
Csx/Nkx-2.5
- DMSO
+ DMSO
M 0 4 8 12 4 8 12
GATA-4
- DMSO
+ DMSO
M 0 4 8 12 4 8 12
α-MHC
- DMSO
+ DMSO
M 0 4 8 12 4 8 12
MLC-2v
- DMSO
+ DMSO
M 0 4 8 12 4 8 12

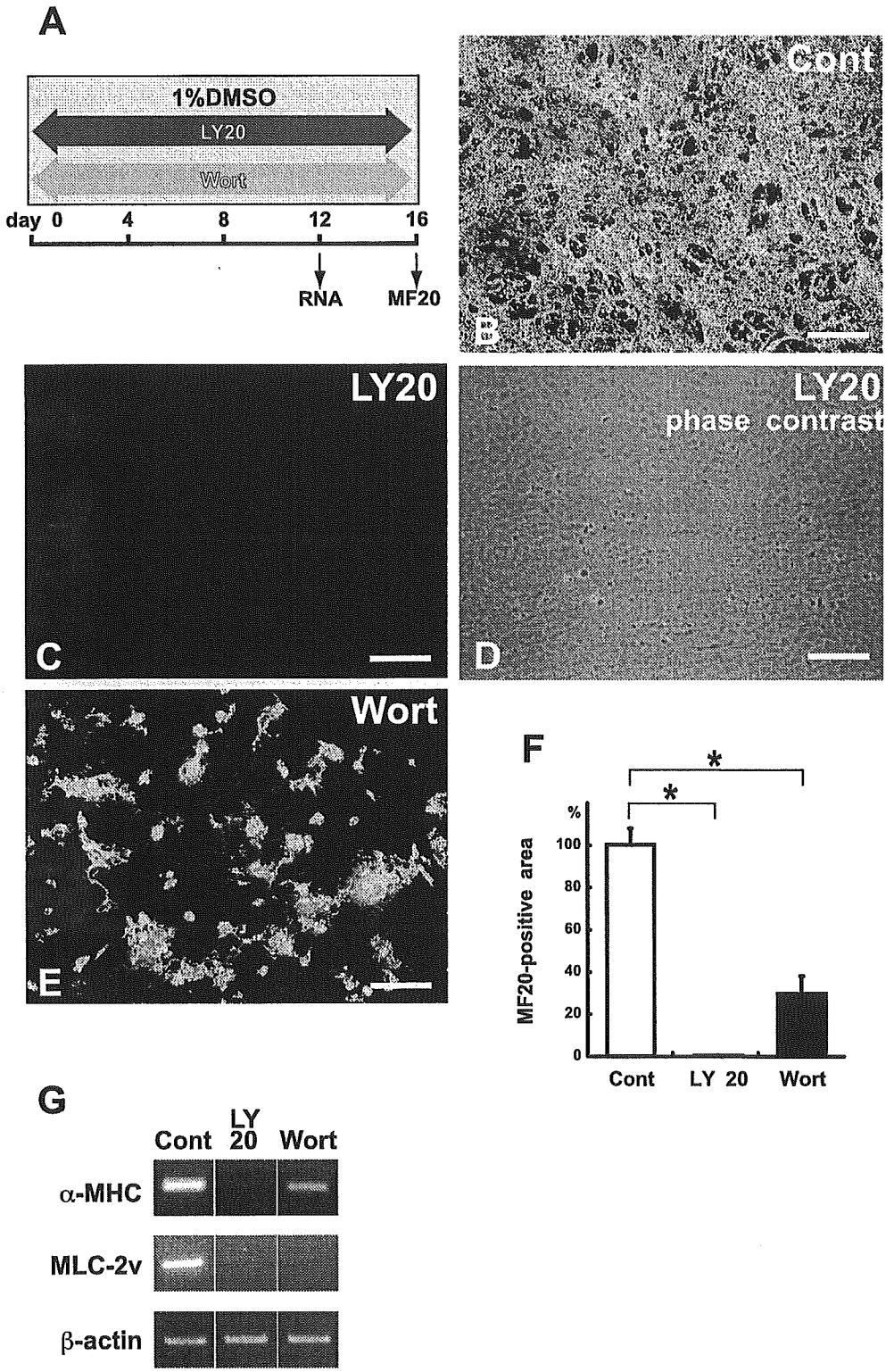

Fig. 2. Inhibition of cardiomyocyte differentiation of P19CL6 cells by PI3-kinase inhibitors. Schematic diagram of the experiment (A). Differentiation of P19CL6 cells was induced as described in the legend for Fig. 1, but the cells were exposed to LY294002 (20 μM) or wortmannin (1 μM) during the time periods delimited by the arrows. On day 16, cells were stained with MF20 (B, C, and E). P19CL6 cells cultured in differentiation medium without PI3-kinase inhibitors (Cont) (B). P19CL6 cells cultured in differentiation medium containing 20 μM LY294002 (LY20) (C). Phase-contrast photomicrograph of the same

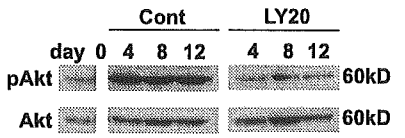

Fig. 3. Activation of PI3-kinase during cardiomyocyte differentiation of P19CL6 cells and suppression of activation by LY294002. Protein was extracted on days 4, 8, and 12 from P19CL6 cells cultured in differentiation medium containing 0 or 20 μM LY294002 (Cont, LY20). Protein samples were also extracted from undifferentiated P19CL6 cells on day 0. Phosphorylated Akt at serine 473, which was used as an indicator for PI3-kinase activity, was measured in each protein sample (40 μg) by Western blotting using phospho-specific Akt (Ser473) (pAkt). The amount of total Akt was determined with a phospho-independent antibody for Akt (Akt).

tinct from LY294002 and inhibits the activity of PI3-kinase by a different mechanism [28]. Since wortmannin is highly unstable in aqueous solutions, we treated P19CL6 cells with relatively high concentration (1 μM) of wortmannin according to the method described in a previous report [10]. When wortmannin was added to the differentiation medium, the MF20-positive area was also decreased (Fig. 2E and F). RT-PCR analysis (Fig. 2G) revealed that treatments with wortmannin suppressed the α-MHC gene expression and completely inhibited the expression of MLC-2v. Treatment with LY294002 at 20 μM totally abolished the expression of these genes. These results suggest that PI3-kinase inhibitors suppressed cardiomyocyte differentiation through specific inhibition of PI3-kinase activity and that PI3-kinase plays a pivotal role in cardiomyocyte differentiation.

Activation of PI3-kinase in differentiation-induced P19CL6 cells and suppression of activation by LY294002

To investigate whether PI3-kinase is activated during cardiomyocyte differentiation of P19CL6 cells, we used phosphorylation of Akt at serine 473 as a marker for activation of PI3-kinase, because extensive research has shown that phosphorylation at this site reflects the activity of PI3-kinase [29,30]. Whereas only a small amount of phosphorylated Akt was detected before induction of differentiation, a greater amount was found after induction, and the phosphorylation was maintained throughout the differentiation (Fig. 3). LY294002 treatment at the concentration of 20 μM decreased phosphorylated Akt to the level of undifferentiated P19CL6 cells although the cells were similarly treated with DMSO (Fig. 3). These results indicate that PI3-kinase was activated by inducing cardiomyocyte differentiation and that the activation of PI3-kinase was suppressed by LY294002 treatment.

Stage-specific inhibition of cardiomyocyte differentiation by LY294002

To investigate at which developmental stage LY294002 exerts its inhibitory effect on cardiomyocyte differentiation, P19CL6 cells were treated with LY294002 (20 μM) for 4 consecutive days at various time points during the differentiation process, and differentiation into cardiomyocytes was analyzed by RT-PCR for cardiac contractile protein genes on day 12 and by immunostaining using MF20 on day 16 (Fig. 4A). LY294002 (20 μM) treatment from days 0 to 4 markedly inhibited cardiomyocyte differentiation of P19CL6 cells, and even on day 16 no contracting cardiomyocytes were observed under a microscope. In contrast, 4-day treatment with LY294002 either from days 4 to 8 or from days 8 to 12 had no significant effects on the differentiation of P19CL6 cells, and vigorous spontaneous contraction similar to that in LY294002-untreated control cells was observed in these cells. RT-PCR analysis (Fig. 4B) revealed that the expressions of α-MHC and MLC-2v were completely suppressed in the cells that were treated with LY294002 from days 0 to 4. In the cells that were treated with LY294002 from days 4 to 8 or from days 8 to 12, the expression of α-MHC did not show significant differences compared with the positive control, whereas the expression of MLC-2v was reduced, suggesting that LY294002 had some effects on expression of MLC-2v but no effect on expression of α-MHC.

Immunostaining using MF20 revealed that only a few of the cells that were treated with LY294002 from days 0 to 4 were positive for MF20 (Fig. 4D). Given the complete lack of expression of α-MHC and MLC-2v, the absence of spontaneous beating observed under a microscope, and the fact that MF20 detects not only cardiac but also skeletal sarcomeric MHC, we assumed that the few MF20-positive cells observed after LY294002 treatment from days 0 to 4 (Fig. 4D) were skeletal myocytes. To test this assumption, we performed RT-PCR analysis for the expression of MyoD, a skeletal-muscle-specific transcription factor, in the cells on day 12. MyoD expression was observed only in the cells treated with LY294002 from days 0 to 4 (Fig. 4B). Thus, the few MF20-positive cells observed after LY294002 treatment from days 0 to 4 seem to have been skeletal myocytes. Contrary to the significant suppression of cardiomyocyte differentiation with LY294002 treatment from days 0 to 4,

field as shown in C (D). Note that cells reach confluence. P19CL6 cells cultured in differentiation medium containing 1 μM wortmannin (Wort) (E). Scale bars, 100 μm. Morphometry for the expression of sarcomeric MHC in P19CL6 cells continuously treated with LY294002 (20 μM) or wortmannin (1 μM) for 16 days using MF20 immunostaining (F). Data are expressed as means ± SD for percentage MF20-positive area (pixel × pixel) compared with control P19CL6 cells cultured in differentiation medium without PI3-kinase inhibitors. At least four different fields were measured for each dish. *Significantly different from control PI3-kinase inhibitor-untreated cells (Dunnett's test). Expression of α-MHC, MLC-2v, and β-actin (G) in P19CL6 cells continuously treated with LY294002 (20 μM) (LY20) or wortmannin (1 μM) (Wort) for 12 days measured by RT-PCR. RNA was extracted from the cells on day 12 and analyzed by RT-PCR as described under Materials and Methods. Expression of β-actin is shown as an internal control.

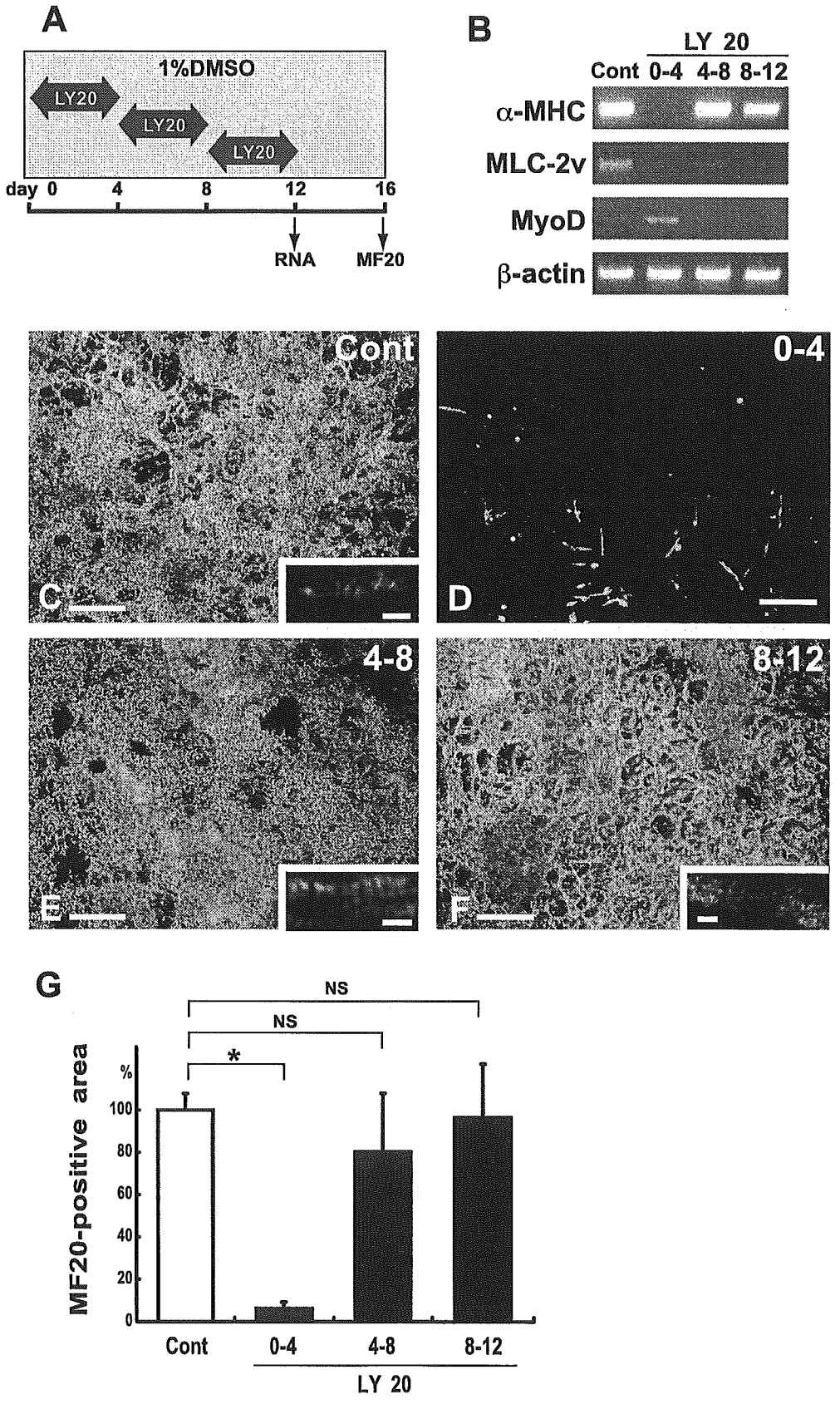
A
1%DMSO
LY20
LY20
LY20
day 0
4
8
12
16
RNA
MF20
B
LY 20
Cont 0-4 4-8 8-12
α-MHC
MLC-2v
MyoD
β-actin
Cont
0-4
4-8
8-12
C
D
E
F
G
NS
NS
*
MF20-positive area
%
100
80
60
40
20
0
Cont
0-4
4-8
8-12
LY 20

LY294002 treatment from days 4 to 8 (Fig. 4E) or from days 8 to 12 (Fig. 4F) had no significant effects on the expression of sarcomeric MHC detected by MF20 (Fig. 4G). The cells that were treated with LY294002 from days 0 to 4 showed no spontaneous beating cells even on day 21 (data not shown), indicating that the inhibitory effects of LY294002 on cardiomyocyte differentiation of P19CL6 cells at a very early stage were irreversible.

Dose-dependent early stage-specific inhibition of cardiomyocyte differentiation of P19CL6 cells by LY294002

To further confirm that the inhibitory effect of LY294002 during the first 4 days was due to specific inhibition of PI3-kinase activity, we treated P19CL6 cells with two different concentrations (10 and 20 μM) of LY294002 from days 0 to 4 (Fig. 5A). We analyzed PI3-kinase activity by phosphorylation of Akt on day 4 and differentiation into cardiomyocytes by immunostaining using MF20 on day 16. LY294002 treatment from days 0 to 4 had dose-dependent inhibitory effects both on phosphorylation of Akt (Fig. 5B) and on the expression of sarcomeric MHC (Fig. 5C–F). Thus, LY294002 apparently inhibits cardiomyocyte differentiation of P19CL6 cells by specific blocking of PI3-kinase activity during the first 4 days of differentiation.

Suppression of Csx/Nkx-2.5 and GATA-4 expression in LY294002-treated cells

Based on the observation that activation of PI3-kinase during the first 4 days is required for cardiomyocyte differentiation, we hypothesized that PI3-kinase influences cardiomyocyte differentiation by modulating the expression of the cardiac transcription factors Csx/Nkx-2.5 and GATA-4 during the first 4 days of differentiation. To test this hypothesis, we treated P19CL6 cells with LY294002 at two different concentrations (10 and 20 μM) and analyzed the expression of Csx/Nkx-2.5 and GATA-4 by semiquantitative RT-PCR on day 4 (Fig. 6A). Both Csx/Nkx-2.5 and GATA-4 were expressed in differentiation-induced P19CL6 cells in the absence of LY294002. LY294002 treatment dose-dependently inhibited the expression of both Csx/Nkx-2.5 and GATA-4 (Fig. 6A and B). Csx/Nkx-2.5 and GATA-4 expression was strongly inhibited by LY294002 treatment at 10 μM and almost completely abolished by LY294002 treatment at 20 μM (Fig. 6B). Together with the results for Akt phosphorylation (Fig. 5B), these data reveal that LY294002 simultaneously suppressed the activation of PI3-kinase and the expression of Csx/Nkx-2.5 and GATA-4. These findings suggest that PI3-kinase regulates cardiomyocyte differentiation by modulating the expression of cardiac transcription factors.

Effects of LY294002 on cell proliferation and apoptosis in P19CL6 cells

BrdU labeling analysis at 0, 24, and 48 h showed that the effects of LY294002 on cell proliferation were time-dependent, i.e., LY294002 significantly reduced BrdU-labeling indexes at 24 h irrespective of DMSO treatment, whereas it increased BrdU-labeling indexes at 48 h (Fig. 7A).

TUNEL assay at 0, 24, and 48 h demonstrated that the effects of LY294002 on apoptosis were different in DMSO-treated and -untreated cells. At 24 and 48 h, LY294002 dose-dependently increased TUNEL indexes after cardiomyocyte induction by DMSO, whereas in untreated cells LY294002 treatment had no significant effects on TUNEL indexes (Fig. 7B).

Discussion

The present study using an in vitro differentiation system of P19CL6 cells revealed that the PI3-kinase pathway plays a pivotal role at a very early stage of cardiomyocyte differentiation. In our experiment, the PI3-kinase pathway was activated by inducing cardiomyocyte differentiation and cardiomyocyte differentiation was blocked by PI3-kinase inhibitors. We also found that LY294002 treatment restricted to the interval from days 0 to 4 was sufficient to inhibit cardiomyocyte differentiation in a dose-dependent manner and completely abolished the differentiation at the concentration of 20 μM. In contrast, LY294002 treatment (20 μM) either from days 4 to 8 or from days 8 to 12 produced no significant changes in the expression of sarcomeric MHC. In addition, we found that the expression of Csx/Nkx-2.5 and GATA-4 was also suppressed by

Fig. 4. Stage-specific inhibition of cardiomyocyte differentiation of P19CL6 cells by LY294002. Schematic diagram of the experiment (A). Differentiation of P19CL6 cells was induced as described in the legend for Fig. 1, but the cells were treated with LY294002 (20 μM) for the 4 days delimited by the arrows. Expression of α-MHC, MLC-2v, MyoD, and β-actin (B) in P19CL6 cells treated with 20 μM LY294002 from days 0 to 4 (0–4), from days 4 to 8 (4–8), or from days 8 to 12 (8–12) or without LY294002 (Cont), measured by RT-PCR. RNA was extracted from the cells on day 12 and analyzed by RT-PCR as described under Materials and Methods. Expression of β-actin is shown as an internal control. Cells were treated with LY294002 (D–F) at the indicated time period and stained with MF20 on day 16. Cells without LY294002 treatment (Cont) (C). Cells were treated with LY294002 from days 0 to 4 (D), from days 4 to 8 (E), or from days 8 to 12 (F). Scale bars, 100 μm. Insets: Higher magnification reveals cross striations. Scale bars, 2 μm. Morphometry for the expression of sarcomeric MHC (G) in P19CL6 cells treated with LY294002 (20 μM) for 4 days using MF20 immunostaining. Data are expressed as means ± SD for percentage MF20-positive area (pixel × pixel) compared with control P19CL6 cells cultured in differentiation medium without LY294002. At least four different fields were measured for each dish. *Significantly different from the control LY294002-untreated cells; NS, no significant difference from the control LY294002-untreated cells (Dunnett's test).

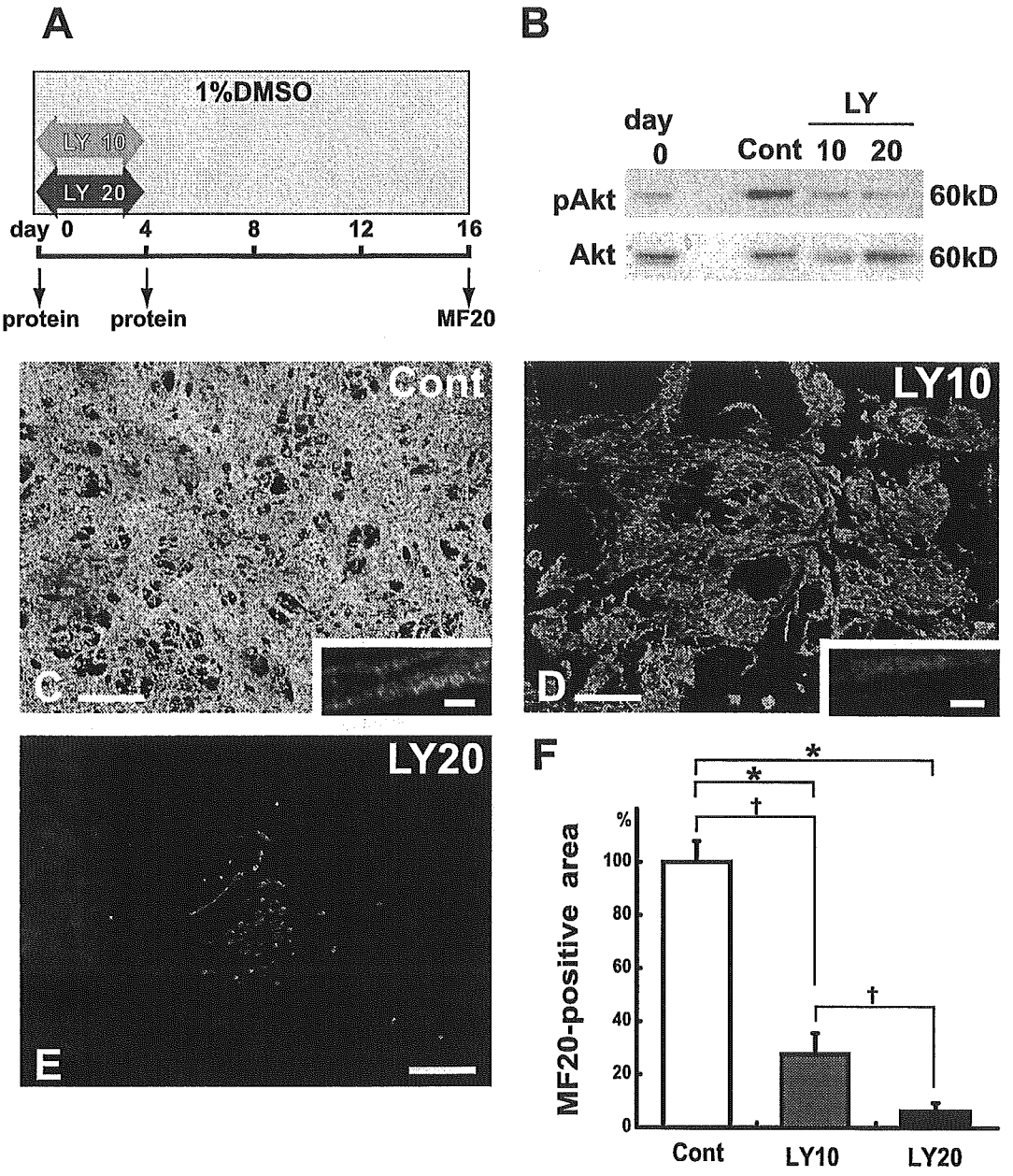

Fig. 5. Dose-dependent early stage-specific inhibition of cardiomyocyte differentiation of P19CL6 cells by LY294002. Schematic diagram of the experiment (A). Differentiation of P19CL6 cells was induced as described in the legend for Fig. 1, but LY294002 was added at 10 or 20 μM (LY10 or LY20) during the first 4 days. P19CL6 cells were cultured in differentiation medium that contained 0, 10, or 20 μM LY294002 (Cont, LY10, and LY20) and protein was extracted on day 4 (B). Protein samples were also extracted from undifferentiated P19CL6 cells on day 0. Phosphorylated Akt at serine 473 in each protein sample (40 μg) was measured by Western blotting using phospho-specific Akt (Ser473) (pAkt). The same blots were stripped and incubated with a phospho-independent antibody for Akt. Cells were treated with LY294002 at concentrations of 0, 10, and 20 μM (C–E) from days 0 to 4 and stained with MF20 on day 16. Positive control P19CL6 cells cultured in differentiation medium without LY294002 (Cont) (C). Cells treated with 10 μM LY294002 (LY10) from days 0 to 4 (D); cells treated with 20 μM LY294002 (LY20) from days 0 to 4 (E). Scale bars, 100 μm. Insets: At higher magnification cross striations are visible. Scale bars, 2 μm. Morphometry for the expression of sarcomeric MHC (F) in P19CL6 cells treated with LY294002 at 10 or 20 μM (LY10 or LY20) from days 0 to 4. Data are expressed as mean ± SD for percentage MF20-positive area (pixel × pixel) compared with control P19CL6 cells cultured in differentiation medium without LY294002 (Cont). At least four different fields were measured for each dish. *Significantly different from the control LY294002-untreated cells (Cont) by Dunnett's test; †significantly different by the Tukey–Kramer test.

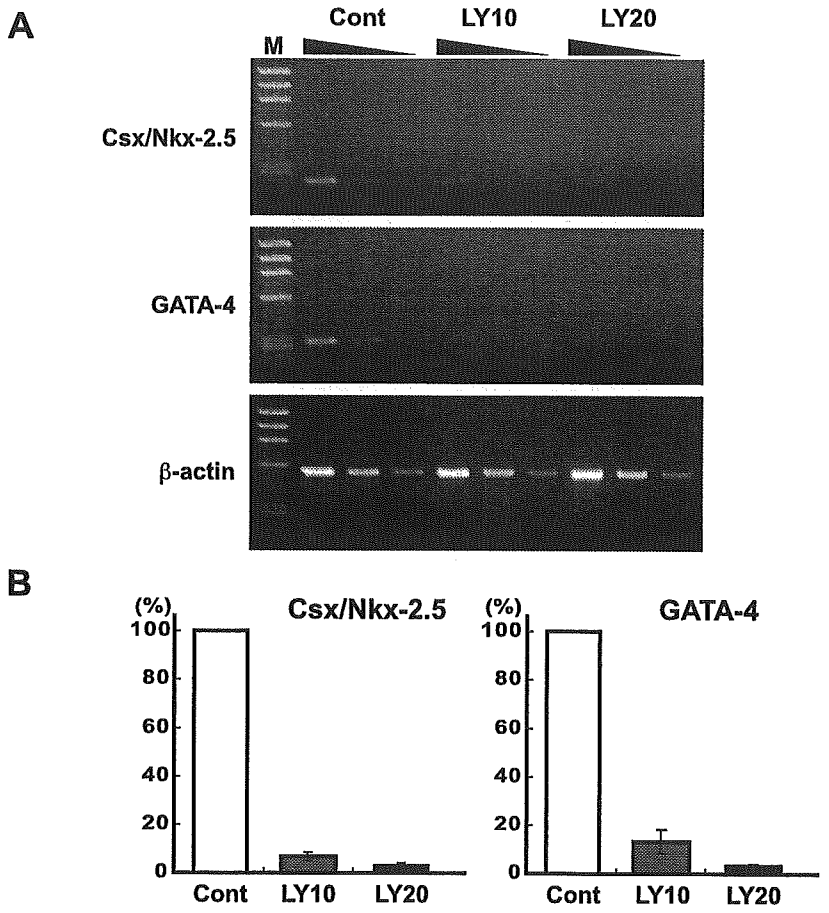

Fig. 6. Semiquantitative RT-PCR showing suppression of expression of Csx/Nkx-2.5 and GATA-4 by LY294002 treatment. Differentiation of P19CL6 cells was induced as described in the legend for Fig. 1, but LY294002 was added at 0, 10, or 20 μM during the first 4 days (A). On day 4, RNA was extracted from LY294002-treated (LY10 and LY20) and LY294002-untreated (Cont) P19CL6 cells and cDNA was synthesized from 1 μg of RNA. PCR was carried out on undiluted cDNA and on fourfold serial dilutions of cDNA, as indicated by the descending wedges. The gene products were analyzed by agarose gel electrophoresis and stained with ethidium bromide. M, molecular weight marker (ϕX 174/*Hae*III). Expression of β-actin is shown as an internal control. Quantitation of the levels of mRNAs (B) in LY294002-treated P19CL6 cells relative to LY294002-untreated P19CL6 cells. The relative expression levels in different samples were determined by calculating the fold dilution of the undiluted positive control cDNA which would be required for similar signal intensities. Data are expressed as means ± SD for percentage Csx/Nkx-2.5 and GATA-4 expression compared with control P19CL6 cells cultured in differentiation medium without LY294002 (Cont).

LY294002 treatment from days 0 to 4 in a dose-dependent manner, suggesting that the PI3-kinase pathway regulates cardiomyocyte differentiation by modulating the expression of cardiac transcription factors.

These data obtained after LY294002 treatment not only confirmed the inhibitory effects of LY294002 on cardiomyocyte differentiation observed by Klinz et al. [18] and by Sauer et al. [19] using ES cells but also clarified that PI3-kinase activation is required only at a very early stage in cardiomyocyte differentiation, i.e., during the first 4 days. As described in the Introduction, early cardiomyocyte differentiation can be divided into three stages, i.e., the precardioblast stage, cardioblast stage, and cardiomyocyte stage. Although Klinz et al. [18] and Sauer et al. [19] had reported that LY294002 suppressed cardiomyocyte differentiation, the stage at which PI3-kinase plays its crucial role in cardiomyocyte differentiation remained unknown. The reason is that in their studies, ES cells were treated with LY294002 from days 3 to 7, during which period the whole set of differentiation processes, i.e., cardiac lineage commitment, proliferation and differentiation of cardioblasts, and maturation and maintenance of cardiomyocytes, occurred, and thus the particular stage influenced by PI3-kinase could not be investigated. On the other hand, the present work is novel in that it identifies the period during which LY294002 treatment exerts its effects on suppression of cardiomyocyte differentiation.

Our finding that LY294002 treatment from days 0 to 4, but not from days 4 to 8 nor from days 8 to 12, suppressed cardiomyocyte differentiation suggests that PI3-kinase plays its important role in cardiomyocyte differentiation mainly at the cardioblast stage after cardiac lineage com-

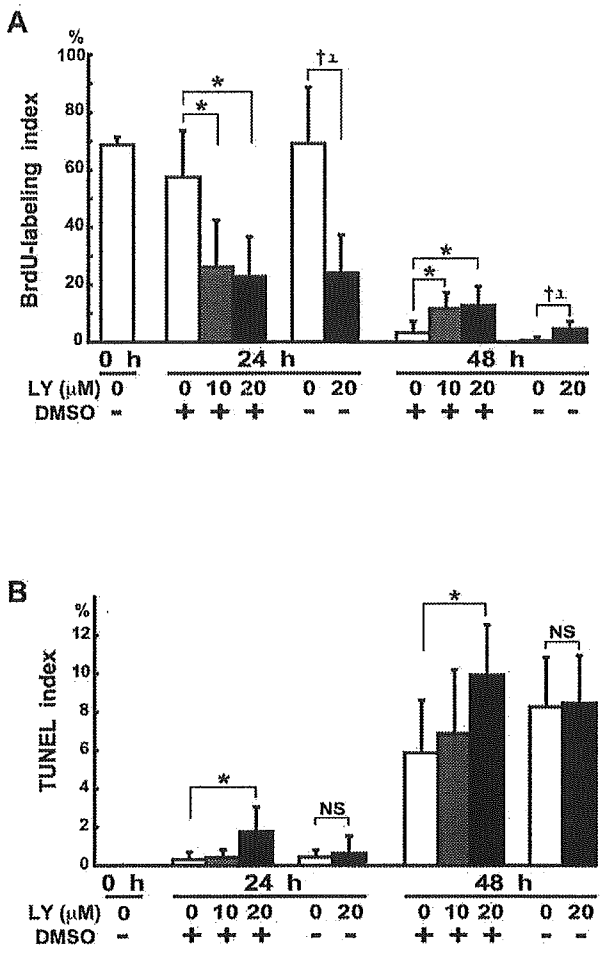

Fig. 7. Effects of LY294002 on cell proliferation and apoptosis in P19CL6 cells. Morphometric data on the BrdU-labeling index, i.e., the number of BrdU-positive nuclei per the number of total nuclei stained with PI (A) and TUNEL index, i.e., the number of TUNEL-positive nuclei per the number of total nuclei stained with PI (B). Two different series of experiments were performed and at least five different fields were measured for each dish. Values represent the mean ± SD. *Significantly different by the Tukey–Kramer test; †significantly different by the Mann–Whitney *U* test; NS, no significant difference (Mann–Whitney *U* test).

mitment, rather than at the cardiomyocyte stage. This is because during the period from days 0 to 4 after induction of cardiomyocyte differentiation, the expression of Csx/Nkx-2.5 and GATA-4, but not that of α-MHC or MLC-2v, was induced in P19CL6 cells; this period corresponds to the cardioblast stage. Furthermore, the data showing that Csx/Nkx-2.5 and GATA-4 expression was dose-dependently suppressed by LY294002 treatment indicate that cardiac lineage commitment and the subsequent events were affected by LY294002 treatment. Moreover, the significance of PI3-kinase in the early phase of the differentiation program identified in this study is consistent with the results found for differentiation of other cell lineages including skeletal muscle [11,12], adipocytes [14], and erythroid cells [15]. Even though the main contribution of PI3-kinase occurs during the very early stage of cardiomyocyte differentiation, we also note that in P19CL6 cells that were treated with LY294002 from days 4 to 8 or from days 8 to 12, the expression of MLC-2v was reduced, suggesting that the PI3-kinase pathway also plays some role in maturation of cardiomyocytes.

Our finding that LY294002 treatment at 20 μM during the first 4 days completely inhibited cardiomyocyte differentiation of P19CL6 cells even on day 21 indicates that this inhibition is irreversible and that the first 4 days are a crucial period in cardiomyocyte differentiation. The importance of the first 4 days in cardiomyocyte differentiation of P19CL6 cells was also underscored by the fact that DMSO treatment limited to the first 4 days was sufficient for cardiomyocyte differentiation of P19CL6 cells [31]. In our study, on day 16, there was no significant difference between the MF20-positive areas after 4-day and after 16-day DMSO treatment (data not shown), indicating that inductive roles of DMSO in cardiomyocyte differentiation are limited to the first 4 days of differentiation. It is likely that LY294002 treatment at 20 μM irreversibly inhibits certain crucial events otherwise promoted by DMSO during the first 4 days. On the other hand, obviously DMSO is not the physiological inducer of cardiomyogenesis. Monzen et al. [21] showed using this P19CL6 cell system that unknown DMSO-inducible factors independent of BMP signaling are necessary for the terminal differentiation, because activation of BMP signaling alone is not sufficient to induce cardiomyocyte differentiation in the absence of DMSO. Since these unknown factors are very likely to be induced and play an essential role in the normal development as well, the identification of signals induced by DMSO in this system will probably provide new insights into the regulatory mechanisms of early cardiomyocyte differentiation.

Although we have no detailed experimental data on the mechanism by which LY294002 treatment inhibits the expression of Csx/Nkx-2.5 and GATA-4, several possibilities can be considered. First, PI3-kinase may directly regulate the expression of Csx/Nkx-2.5. There is growing evidence that the BMP–Smad pathway is involved in the induction and expression of Csx/Nkx-2.5 in cardiomyocyte differentiation [22,32]. Moreover, in osteoblast differentiation, cross-talk between the BMP–Smad and PI3-kinase pathways has been reported, i.e., PI3-kinase is activated upon BMP stimulation and positively regulates BMP–Smad signaling through translocation of Smad protein into the nucleus [33]. By analogy, PI3-kinase could regulate Csx/Nkx-2.5 expression through the BMP–Smad pathway during cardiomyocyte differentiation.

Second, PI3-kinase may be involved in the transcriptional loop between Csx/Nkx-2.5 and GATA-4. The importance of this transcriptional loop during cardiomyocyte differentiation has been demonstrated in P19 cells [34,35] and in *Drosophila* [36]. For example, in P19 cells, researchers found that dominant-negative Csx/Nkx-2.5 completely